Proc. Natl. Acad. Sci. USA
Vol. 92, pp. 315–319, January 1995
Immunology

Human immunodeficiency virus (HIV) antigens: Structure and serology of multivalent human mucin MUC1–HIV V3 chimeric proteins

(principal neutralizing determinant/multivalent antigen)

J. DARRELL FONTENOT*, JOE M. GATEWOOD†, S. V. SANTHANA MARIAPPAN*, CHOU-PONG PAU‡, BHARAT S. PAREKH‡, J. RICHARD GEORGE‡, AND GOUTAM GUPTA*§

*Theoretical Biology and Biophysics, T-10, MS-K710, †Life Sciences Division, LS-2, MS 880, Los Alamos National Laboratory, Los Alamos, NM 87545; and ‡Division of HIV/AIDS, National Center for Infectious Diseases, Centers for Disease Control and Prevention, 1600 Clifton Road, Atlanta, GA 30330

Communicated by Hans Frauenfelder, Los Alamos National Laboratory, Los Alamos, NM, September 23, 1994 (received for review May 26, 1994)

ABSTRACT **Molecular modeling and two-dimensional NMR techniques enable us to identify structural features in the third variable region (V3) loop of the human immunodeficiency virus (HIV) surface glycoprotein gp120, in particular the principal neutralizing determinant (PND), that remain conserved despite the sequence variation. The conserved structure of the PND is a solvent-accessible protruding motif or a knob, structurally isomorphous with the immunodominant knobs in the tandem repeat protein of human mucin 1 (MUC1) (a tumor antigen for breast, pancreatic, and ovarian cancer). We have replaced the mucin antigenic knobs by the PND knobs of the HIV MN isolate in a set of chimeric human MUC1/HIV V3 antigens. This produced multivalent HIV antigens in which PNDs are located at regular intervals and separated by extended mucin spacers. In this article we show by two-dimensional NMR spectroscopy that the multivalent antigens preserve the PNDs in their native structure. We also demonstrate by ELISA that the antigens correctly present the PNDs for binding to monoclonal antibodies or polyclonal antisera from HIV-infected patients.**

Fusion of a viral surface with the host-cell surface is the first step in the life cycle of the human immunodeficiency virus (HIV). The process of HIV fusion into a host cell is determined by two discrete functional sites on the 120-kDa viral surface unit glycoprotein, gp120. First, a segment near the C terminus of gp120 directly binds to the CD4 molecule on the surface of a host cell (1, 2). Next, the third variable region (V3) loop of gp120 mediates in virus fusion (3, 4). Virus fusion is abrogated when these binding events are prevented by blocking either one or both of these sites of gp120. The blocking of these sites is the primary mechanism of virus neutralization by antibodies (5–7). Two approaches have been used for viral neutralization: (*i*) vaccination aimed at generating antibodies specific for the principal neutralizing determinant (PND), which is located inside the V3 loop of gp120 and contains a fairly conserved Gly-Pro-Gly-(Arg or Gln) (GPGR/Q) crest at the center of the PND (6, 8); and (*ii*) the administration of soluble CD4 receptors (9). However, these approaches currently suffer from serious drawbacks. For example, because of sequence variability in the V3 loop (8, 10), neutralizing antibodies elicited by the V3 loop from one HIV isolate do not neutralize other HIV isolates (11, 12). Further, the short half-life of soluble CD4 molecules has limited applicability for the treatment of a "slow" virus infection.

The V3 loop of HIV surface gp120 is a potential target for protective immunity. This small 34- to 36-residue domain contains the well-characterized PND as well as a cross-reactive cytotoxic T-lymphocyte epitope (13). The V3 loop also participates in vital functional properties of HIV-like cell tropism (14, 15) and cell fusion (3, 4, 16). Antibody binding to the V3 loop can interfere with these processes in the life cycle of the virus. To exploit the V3 loop as an antibody target, one has to understand (*i*) the effect of sequence variability on the structure and antigenicity and (*ii*) the structural features of the V3 loop (especially at the PND) that remain invariant. Our previous work using theoretical studies of 30 different V3 loops (17, 18) and three-dimensional (3-D) structure determination of two divergent cyclic V3 loops (19, 20) allows us to define the effect of sequence variability on the global structure of the entire V3 loop and the local structure of the PND centered around the conserved GPGR crest. Irrespective of the variability in the amino acid sequences on either side of the type II GPGR turn, the PNDs of different V3 loops adopt a protruding solvent-accessible motif (19–22) or knob. This work focuses on synthetic polypeptide antigens that contain PNDs that preserve and present the same conserved structural features as in the "native" V3 loop. Such a design requires a polypeptide construct that also contains a protruding motif like the PNDs in the V3 loop. The tandem repeat protein, human mucin 1 (MUC1) (a tumor antigen for breast, pancreatic, and ovarian cancer), provides us with such a structural motif (23–25). We construct a set of chimeric human MUC1–HIV V3 loop proteins in which HIV PNDs replace the immunodominant knobs of MUC1 tandem repeats. We show by two-dimensional (2-D) NMR that the PNDs in the chimeric proteins preserve the same structure as in the native V3 loops. Finally, we show that these antigens are also able to bind polyclonal antisera from HIV-infected patients and type-specific monoclonal antibodies (mAb).

MATERIALS AND METHODS

The 60- and 120-residue peptide amides were synthesized, and the products of the synthesis were deprotected, cleaved from the resin support, purified by HPLC, and subjected to molecular weight determination by electrospray mass spectroscopy as described (26). The names and sequences in single-letter amino acid code of one copy of the tandem repeat antigens described here are as follows: human MUC1, VTSAPDTRPAPGSTAPPAHG; MUC1–V3 1.1, VTSGPGRAFAPGSTAPPAHG; MUC1–V3 1.2, HIGPGRAPAPGSTAPPAHGV;

The publication costs of this article were defrayed in part by page charge payment. This article must therefore be hereby marked "*advertisement*" in accordance with 18 U.S.C. §1734 solely to indicate this fact.

Abbreviations: HIV, human immunodeficiency virus; PND, principal neutralizing determinant; NOE, nuclear Overhauser effect; NOESY, NOE spectroscopy; gp120, 120-kDa glycoprotein; V3, variable region third loop of HIV surface gp120; mAb, monoclonal antibody; MUC1, human mucin 1; GPGR/Q, Gly-Pro-Gly-(Arg or Gln); 2-D and 3-D, two- and three-dimensional; HIGPGRA, His-Ile-Gly-Pro-Gly-Arg-Ala.

§To whom reprint requests should be addressed.

and MUC1–V3 1.3, IHIGPGRAFAPGSTAPPAHG. In each case, peptides with three and six complete tandem repeats were successfully synthesized. The cyclic and linear V3 peptides from the HIV isolate MN (HIV-MN) have the single-letter-code sequence CTRPNYNKRKRIHIGPGRAFYTTK-NIIGTIRQAHC, and the small 15-residue linear peptide has the sequence DKRIHIGPGRAFYTT. The enzyme-linked immunosorbent assay (ELISA) was performed as described (27).

All NMR experiments on the MUC1–V3 60-residue antigen were carried out on the 600-MHz Bruker spectrometer at the University of Alabama at Birmingham. All NMR spectra were collected at 10°C with peptide concentration at 5 mM (pH 5.5). All 2-D data were acquired in the phase-sensitive mode with the presaturation of the $^1H^2HO$ signal during the relaxation delay (28, 29).

As previously described (18, 19), a set of distance constraints were derived by analyzing the NMR data with the aid of full-matrix nuclear Overhauser effect (NOE) spectroscopy (NOESY) simulations, associated *R*-factor test, and energy calculations. Analyses of the 2-D NMR data of the MUC1–V3 60-residue peptide produced 220 interproton distance constraints. The energy term EDIST (14, 38) was added to the force-field as described by Scheraga and coworkers (30). Monte Carlo-simulated annealing (31) was performed to obtain a set of structures consistent with NMR data. The maximum step size of the torsion angles was set at 15 degrees, which produced an acceptance ratio of 0.20–0.50 for the 50,000-step Monte Carlo cycle at each temperature. Full-matrix NOESY calculations were repeated for the final 150 low-energy MUC1–V3 structures. These structures were analyzed in terms of their energies, end-to-end lengths (R_e), relative orientations of the knobs, and torsion angle parameters.

RESULTS

Principles of Design. We previously determined NMR structures of two disulfide-bridged V3 loops: a Thailand HIV isolate (19) and the HIV-MN isolate (38). Amino acid sequences of the PNDs of these two V3 loops are quite different. However, as shown by superimposing two PNDs (Fig. 1 *Left*), both of them form similar protruding motifs. In the case of the HIV Thailand isolate, the central GPGQ forms a type II turn and a solvent-accessible tip; similarly in the case of HIV-MN, the central GPGR forms the type II turn and the accessible tip. In spite of the fact that the amino acid sequences flanking the central type II turn on the N- and C-terminal sides are different, the polypeptide backbone and side-chain orientations in the flanking regions are very similar in the two cases (Fig. 1 *Left*). However, when the PND is presented in the context of the V3 loop or gp120, the variability of regions flanking the central PND residues masks the conformational purity of the PND.

These protruding motifs (or knobs) are predicted from molecular modeling studies (17, 18) of a large set of different V3 loops. The "knob-like" structure is also present in the tandem repeat domain of a protein totally unrelated to HIV V3 loops. Fig. 1 *Right* illustrates the surprising result found upon solving the structure of three tandem repeats of the human breast and pancreatic tumor antigen MUC1, (PDTRPAPGSTAPPAHGVTSA)$_3$. In this system, we again found a knob-like motif that is crested by a type II turn (isomorphous with the PND of HIV), which is immunodominant for humoral immune responses (32, 33). As shown by detailed NMR analyses (25), the elongated mucin structure contains knobs that project away from the long axis of the molecule and are connected by extended spacers (Fig. 1 *Right*). In the mucin structure, Ala-Pro-Asp-Thr from positions 0–3 in the above repeat (where Ala at position 0 is the amino acid from the previous repeat) forms the type II turn occupying the solvent-accessible tip of the knob; this tip is the immunodominant antigenic site in MUC1. In our antigen-engineering approach, we chemically synthesize a series of MUC1–V3 chimeric polypeptides in which mucin immunodominant knobs are replaced by the HIV-MN PNDs (Fig. 1 *Right*). The ability of these chimeric proteins to act as HIV antigens requires fulfillment of two criteria: (*i*) the PNDs in MUC1–V3 antigens

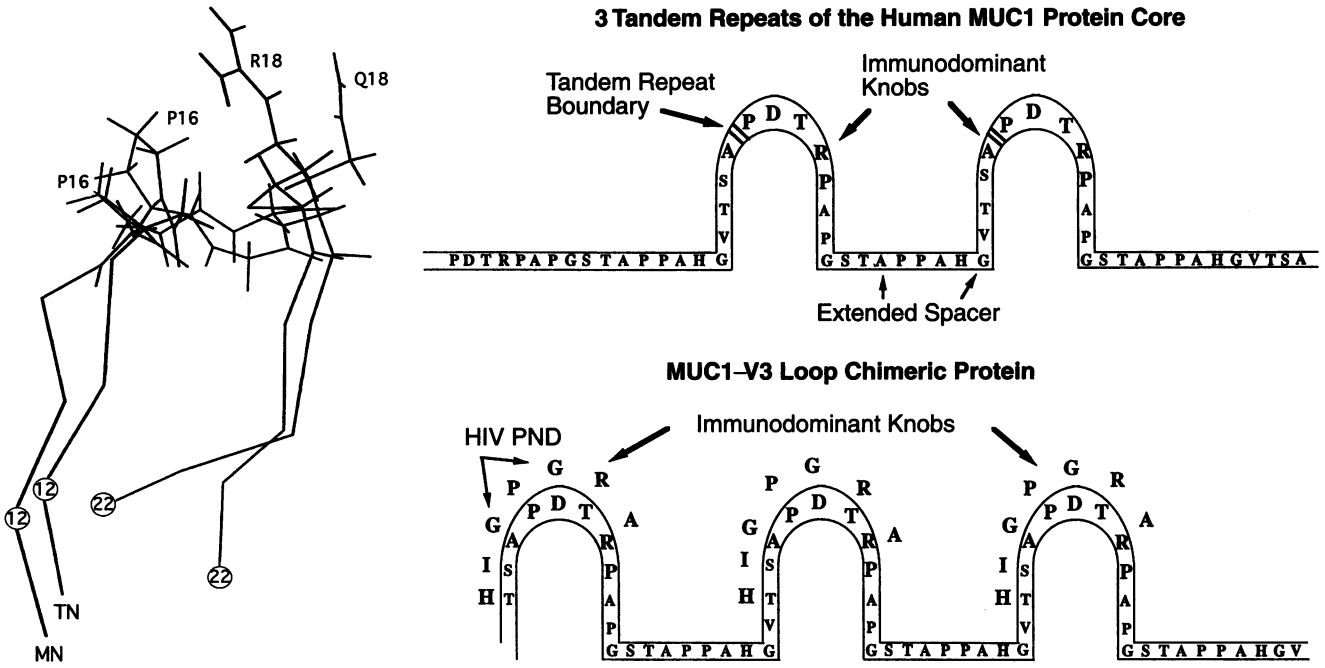

FIG. 1. (*Left*) Superimposition of the protruding motifs of two NMR structures: the V3 loop from the HIV-MN isolate (designated MN) and that from the Thailand TN243 isolate (named TN). The sequences of two motifs in single-letter amino acid code are: MN, RIHIGPGRAFYT; and TN, SITIGPGQVFYR. Note that the GPGR or GPGQ crests are oriented in the same way. (*Right*) The principle of design. The HIV PND sequences above the MUC1 sequences actually replace the MUC1 residues in the chimeras.

must be structurally equivalent with the native V3 loop, and (*ii*) the surface accessibility to antibodies of the PNDs in MUC1–V3 antigens must be as good as or better than in the native V3 loop. Below, we discuss how these criteria are fulfilled for the MUC1–V3 antigens that we have designed so far.

Preservation of Structure. We have chemically synthesized 60- and 120-residue peptides of three different MUC1–V3 antigens in which three different lengths of HIV-MN PND sequences are inserted. The lengths of the PND inserts are 6, 7, and 9 amino acids. The names and sequences of the chimeric antigens are listed in *Materials and Methods.* The start of the sequence is chosen in such a way that each 20-amino acid repeat has one knob (Fig. 1 *Right*). Therefore, by varying the number of repeats, we can vary the number of knobs and study the related effect on the structure and dynamics of the antigen and on the associated antibody-binding affinity. The binding data indicates that we need at least 7 PND amino acids for optimum binding.

The NOESY (400 ms of mixing) fingerprint region (containing cross-peaks due to coupling between backbone H^N and H^α) of the MUC1–V3 1.2 60-residue peptide reveals that the 20 residues in the sequence repeat also forms the structural repeat—i.e., the protons from the 20 amino acids in all three repeats sample the same chemical-shift environment and structure (Val-60 being the only exception). Comparison of the NOESY cross-section from the MUC1–V3 1.2 60-residue peptide with that of the MUC1–V3 1.2 120-residue peptide suggests that local structures of different 20-amino acid repeats in the same antigen (60 or 120 residue) are remarkably similar. However, the extent of flexibility and the nature of dynamics can be different in these two antigens. The diagnostic NOE pattern of importance is the one involving the HIV PND epitopes, His-Ile-Gly-Pro-Gly-Arg-Ala (HIGPGRA), of MUC1–V3 1.2. The $H^\alpha(P_i)$–$H^N(G_{i+1})$, $H^\alpha(P_i)$–$H^N(R_{i+2})$, and $H^N(G_i)$–$H^N(R_{i+1})$ NOEs are indicative of a type II β-turn of GPGR centered around the proline and glycine residues (19, 34, 35). The sequential NOE pattern involving histidine, isoleucine and alanine residues of HIGPGRA defines the backbone and side-chain orientations of the flanking residues in the PND with respect to the central GPGR type II turn. The NOESY (200 ms of mixing) fingerprint (H^N–H^α) region of MUC1–V3 1.2 120-residue peptide has features similar to those in the MUC1–V3 1.2 60-residue peptide except that the weak $H^\alpha(P_i)$–$H^N(R_{i+2})$ NOE present is not seen.

The analyses of the NMR data of MUC1–V3 1.2 60-residue peptide revealed intraresidue NOEs involving H^α–H^N, H^β–H^N, H^γ–H^N, H^α–H^β, H^β–H^γ, etc., and interresidue NOEs involving H^α(residue i)–H^N(residue $i+1$), $H^\beta(i)$–$H^N(i+1)$, $H^N(i+1)$–$H^N(i+1)$, and some $H^\gamma(i)$–$H^N(i+1)$. Full-matrix analyses and the associated *R*-factor test with respect to the NOESY data at 200 and 400 ms of mixing produced 220 distance constraints for the MUC1–V3 1.2 60-residue peptide (36). Simulated annealing subject to the distance constraints resulted in a set of stable (low energy) structures in agreement with the NMR data. All of the structures shared the following common features: (*i*) a tight GPGR type II turn; (*ii*) a protruding motif (or knob—colored red) consisting of residues 1–11 in each repeat, with the GPGR forming the solvent-accessible tip; (*iii*) seven residues from the HIV-MN PND in MUC1–V3 that are structurally isomorphous with the same residues in the cyclic HIV-MN V3 (Fig. 2); and (*iv*) an extended spacer (colored green), consisting of β-strand and polyproline structures, connecting the knobs. We noticed significant conformational flexibility in the MUC1–V3 1.2 60-residue peptide in terms of the end-to-end length (R_e) and in the relative distance and orientations of the knobs. This flexibility neither violates the NMR distance constraints nor disrupts structural features *i–iv* discussed above. Fig. 3 shows three different folded forms of the MUC1–V3 1.2 60-residue peptide in agreement with the NMR data. Fig. 3 *Left* shows a structure with R_e = 80 Å and with knobs alternating on two sides of the long axis of the molecule, whereas Fig. 3 *Center* shows a structure with R_e = 80 Å but with the knobs located on the same side of the long axis. A more compactly folded structure with R_e = 30 Å and with the first and the third knobs close together is shown in Fig. 3 *Right.* The conformational variants in Fig. 3 involve only minor variations in backbone torsion angles (i.e., small correlated changes produce large cumulative deviations). Also note that some degrees of flexibility possible for the 60-residue peptide may be sterically prohibited for the 120-residue peptide. For example, the progressive extension of the 60-residue chain at the bottom in Fig. 3 to accommodate the 120-residue peptide may be sterically excluded because of the clash of the third and fourth knobs. Therefore, for steric reasons the 120-residue chain has to necessarily unfurl. This implies, even though the local structures of the 20-amino acid repeats may be identical in the

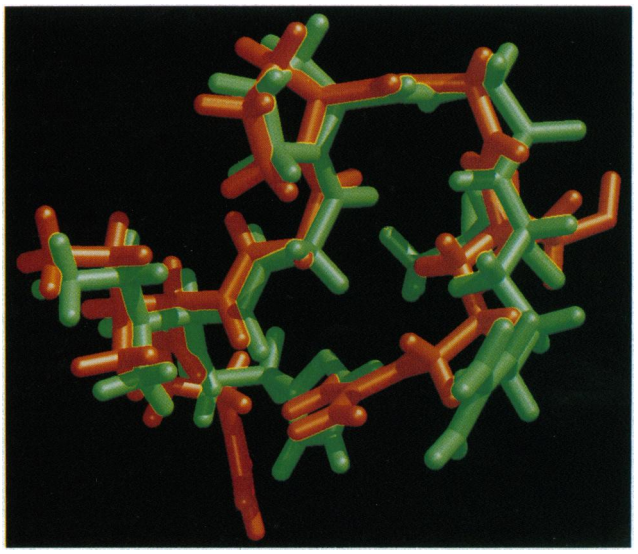

FIG. 2. Structural similarity between the HIV PND isotope HIGPGRA in the HIV-MN cyclic V3 (green) and in the central knob of chimeric MUC1–V3 1.2 60-residue peptide. The residues on the N terminus are on the left, while the residues on the C terminus are on the right. Note that P occupies the left corner of the crest.

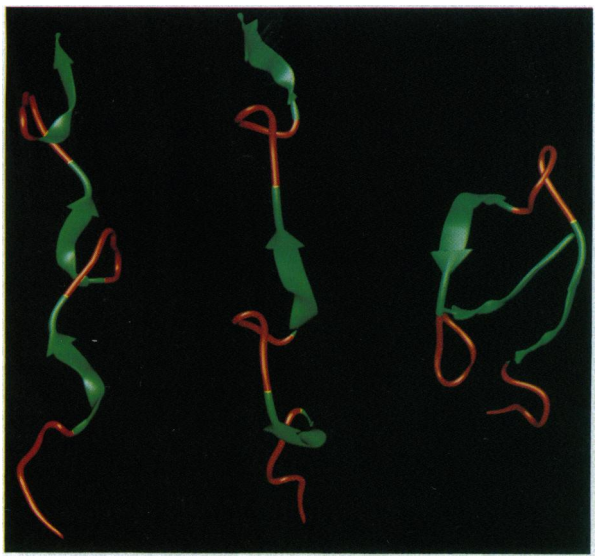

FIG. 3. Flexibility in the arrangement of the tandem repeats in MUC1–V3 1.2 60-residue peptide.

60- and 120-residue peptides, that the global folding and dynamics can be different in these two polypeptides. These differences, in addition to the difference in the number of binding sites, are likely to alter antibody binding properties for these two polypeptides. The results in Figs. 2 and 3 prove that the PND inside the chimeric construct is structurally similar to that in the native V3 loop.

Presentation of Structure. Table 1 lists the ELISA reactivity of various V3 antigens against 39 different polyclonal antisera from HIV-infected patients. Also shown in the table are the PND sequences at the tip of the predominant HIV V3 loops from the corresponding HIV-infected patients. The reactivity of the mucin 105-mer is also shown on a relative scale of 0 to 4 (0 being least reactive). Note that 37 of 39 antisera in Table 1 show no reactivity with the mucin 105-mer; the remaining two show only weak binding. However, MUC1–V3 120-residue antigens show reactivity comparable to the full-length linear and cyclic V3 loops in the majority of the cases. MUC1–V3 1.3, which has the longest PND segment, is the most reactive among all three MUC1–V3 antigens. The conformational purity of the PND epitope in MUC1–V3 1.3 (and not the length of the sequence) decides the high reactivity. By comparison, the 14-residue linear V3 peptide (with 5 more residues than the PND in MUC1–V3 1.3) is much less reactive. This is because the small linear V3 peptide is less structured than the PND in MUC1–V3 1.3. All antisera specific for Ile-Gly-Pro-Gly-Arg-Ala-(±Phe) [IGPGRA(F); i.e., with or without phenylalanine in the epitope] show strong reactivity toward MUC1–V3 1.2. These reactivities compare well with those displayed by the HIV-MN cyclic V3 loop against the same antisera.

Table 1. Reactivity of patient polyclonal antisera and mAbs with V3 antigens

Antibody		Reactivity with V3 antigens						
		HIV-MN V3 loops			MUC1–V3 chimeric 120-residue			Reactivity with mucin 105-mer
Name	V3 loop PND sequence	Cyclic	Linear	Small linear	1.1	1.2	1.3	
HIV patient serum								
HOND01	IPIGPGRAF	+4	+4	+4	+4	+2	+4	+1
HOND02	IHIGPGRAF	+4	+4	+4	+4	+4	+4	0
HOND03	INIGPGRAW	+4	+4	+2	+1	+3	+4	0
HOND04	IHMGPGGAF	+4	+4	0	0	+2	+4	0
HOND05		+4	+4	+4	0	+4	+4	0
HOND06	IYIGPGRAF	+4	+4	+4	+4	+4	+4	0
HOND08	IHIGPGSAW	+4	+4	+2	+1	+4	+4	0
HOND09	IHIGPGRAF	+4	+4	+1	+1	0	+4	0
HOND10	IPIGPGRAF	+4	+4	+4	+4	+4	+4	0
HOND12	IPLGPGRAF	+4	+4	+2	+3	+2	+4	0
HOND13		+4	+4	+4	+3	+4	+4	0
HOND14	IHIGPGRAF	+4	+4	+4	+1	+4	+4	0
HOND15	IHIGPGRAF	+4	+4	+3	+2	+4	+4	0
HOND16	IHIGPGSAW	+4	+4	+4	0	0	+4	0
HOND17	IHIGPGRAF	+4	+4	+4	+1	0	+4	0
HOND18	VTIGPGKVW	+3	+4	+1	0	+3	+4	0
HOND19	INIGPGRAF	+4	+4	+3	+4	+4	+4	0
HOND20		+4	+4	+1	+4	+4	+4	0
HOND51	VHIGPGRAF	+4	+4	+4	+4	+4	+4	0
HOND52	IYIGPGRAF	+4	+4	+4	+4	+4	+4	0
HOND53	VRIGPGRAF	+4	+4	+1	0	0	+1	0
HOND54		+4	+4	+1	0	+4	+4	0
HOND55	INIGPGRAF	+4	+4	+3	0	0	+4	0
HOND58	INIGPGRAF	+4	+4	+4	+4	+4	+4	0
HOND59	VHIGPGRAF	+3	+4	+1	0	0	+2	0
HOND60	INIGPGRAF	+4	+4	+4	+2	+4	+4	0
HOND61		+4	+4	+2	0	+4	+4	0
HOND62		+4	+4	+2	+1	+1	+4	0
RW9223	IHIGPGRAF	+4	+4	+2	+4	+4	+4	0
RW9225	VRIGPGQTF	0	0	0	0	0	+3	0
BR9203	IHMGWGRAF	0	0	0	0	0	0	0
BR9221	IHMGWGRAF	+2	0	0	0	0	0	0
BR9225	IRIGPGQAF	+4	+4	0	0	+1	+3	+2
BR9228	IHMGWGRTF	0	0	0	0	0	0	0
TH9201	INIGPGQVF	0	0	0	0	0	0	0
TH9206	ITIGPGQVF	0	0	0	0	0	0	0
TH9209	ITIGPGQVF	0	0	0	0	0	0	0
UG9238	TPIGQGQVL	0	0	0	0	0	0	0
UG9365	TSIGLGQAL	0	0	0	0	0	+4	0
mAb								
268-D	HIGPGR	+2	+2	—	0	+2	+2	0
R/V3-50.1	RIHIG	+4	+2	—	0	0	+4	0

Reactivity: 0, absorbance A = 1–5× the average of six normal controls; +1, A = 5× the average of six normal controls up to 1.0 A_{405} unit in ELISA; +2, A = 1–1.5 A_{405} units in ELISA; +3, A = 1.5–2.0 A_{405} units in ELISA; +4, A = >2.0 A_{405} units in ELISA.

Two neutralizing mAbs show distinct antigen specificity (Table 1). The human mAb 268-D (12) is specific for the sequence HIGPGR and reacts with MUC1–V3 1.2 and MUC1–V3 1.3 antigens, which contain this sequence, but not with MUC1–V3 1.1, which does not contain this full sequence. The mouse mAb R/V3-50.1, obtained by immunization with a cyclic V3 loop (37), is specific for the sequence Arg-Ile-His-Ile-Gly. This mAb only reacts with MUC1–V3 1.3.

DISCUSSION

MUC1–V3 antigens are unique in the following ways. (*i*) NMR and antibody-binding data verify that they reproduce the native structure of the PNDs even when they are presented in the context of a totally unrelated protein like MUC1. (*ii*) Immunogens containing identical PNDs within the MUC1 chimeras effectively allow enhanced presentation of a conserved structural feature of the virus in a fashion not possible with nonchimeric HIV antigens. The true advantage of this approach will be to induce either T-cell-dependent or T-cell-independent antibody responses to the PND, depending on the precise construction of the antigen. (*iii*) Multiple PNDs, present in these chimeric proteins, may be advantageous in enhancing the immune response by significantly increasing the affinity of antibody binding. The importance of multiple PNDs being present in the same antigen becomes clear by analyzing the relative binding of MUC1–V3 1.2 60- and 120-residue peptides to different antisera. The data show that the 120-residue peptide is a better ligand than the 60-residue peptide for the majority of the antisera we tested (data not shown). This is probably because the higher number of PND knobs in the 120-residue peptides are correctly disposed along the long axis of the molecule to facilitate the binding of bivalent antibodies. (*iv*) Alternatively, the nature of the MUC1–V3 structure (Fig. 3) suggests that if two or more different PNDs are grafted alternately along the chain, there is enough flexibility in the spacers so that two or more antibodies specific for two different PNDs can both bind bivalently, interdigitating along the molecule. Finally, there is no reason why more than two PNDs cannot be introduced in the molecule. This may be critical in designing vaccines for a highly mutating pathogen like HIV.

We acknowledge Dr. Byron Goldstein for his help and encouragement. This work was supported by National Institutes of Health Grant R01 AI32891-01A2 and Los Alamos National Laboratory Grant XL 77; and mAbs were supplied by the National Institutes of Health AIDS Research and Reference Reagent program.

1. Dalgleish, A. G., Beverly, P. C. L., Clapman, P. R., Crawford, D. H., Greaves, M. F. & Weiss, R. A. (1984) *Nature (London)* **312,** 763–766.
2. Robey, E. & Axel, R. (1990) *Cell* **60,** 697–700.
3. Rusche, J. R., Javaherian, K., McDanal, C., Petro, J., Lynn, D. L., Grimaila, R., Langlois, A., Gallo, R. C., Arthur, L. O., Fischinger, P. J., Bolognesi, D. P., Putney, S. D. & Mathews, T. J. (1988) *Proc. Natl. Acad. Sci. USA* **85,** 3198–3202.
4. Freed, E. O., Myers, D. J. & Risser, R. (1991) *J. Virol.* **65,** 190–194.
5. Robert-Guroff, M., Brown, M. & Gallo, R. C. (1985) *Nature (London)* **316,** 72–74.
6. Putney, S. A., Mathews, T. J., Robey, W. G., Lynn, D. L., Robert-Guroff, M., Mueller, W. T., Langlois, A. J., Ghrayeb, J., Jr., S. R. P., Weinhold, K. J., Fishinger, P. J., Wong-Staal, F., Gallo, R. C. & Bolognesi, D. P. (1986) *Science* **234,** 1392–1395.
7. Chamat, S., Nara, P., Berquist, L., Whalley, A., Morrow, W. J. W., Kohler, H. & Kang, C. Y. (1992) *J. Immunol.* **149,** 649–654.
8. LaRosa, G. J., Davide, J. P., Weinhold, K., Waterbury, J. A., Profy, A. T., Lewis, J. A., Langlois, A. J., Dreesman, G. R., Boswell, R. N., Shadduck, P., Holley, L. H., Karplus, M., Bolognesi, D. P., Mathews, T. J., Emini, E. A. & Putney, S. D. (1990) *Science* **249,** 932–935.
9. Chao, B. H., Costopoulos, D. S., Curiel, T., Bertonis, J. M., Chisholm, P., Williams, C., Schooley, R. T., Rosa, J. J., Fisher, R. A. & Marganore, J. M. (1989) *J. Biol. Chem.* **264,** 5812–5817.
10. Myers, G., Korber, B., Berzofsky, J. A., Smith, R. F. & Pavlakis, G. N. (1992) *Human Retroviruses and AIDS* (Los Alamos Natl. Lab., Los Alamos, NM).
11. Matthews, T. J., Langlois, A. J., Robey, W. G., Chang, N. T., Gallo, R. C., Fischinger, P. J. & Bolognesi, D. P. (1986) *Proc. Natl. Acad. Sci. USA* **83,** 9709–9713.
12. Gorny, M. K., Xu, J. Y., Gianakakos, V., Karwowska, S., Williams, C., Sheppard, H. W., Hanson, C. V. & Zolla-Pazner, S. (1991) *Proc. Natl. Acad. Sci. USA* **88,** 3238–3242.
13. Takahashi, H., Nakagawa, Y., Pendleton, C. D., Houghten, R. A., Yokomuro, K., Germain, R. N. & Berzofsky, J. A. (1992) *Science* **255,** 333–336.
14. Hwang, S. S., Boyle, T. J., Lyerly, H. K. & Cullen, B. R. (1991) *Science* **253,** 71–74.
15. Chesebro, B., Wehrly, K., Nishio, J. & Perryman, S. (1992) *J. Virol.* **66,** 6547–6554.
16. Clements, G. J., Price-Jones, M. J., Stephens, P. E., Sutton, C., Schulz, T. F., Clapman, P. R., J. A, M., McClure, M. O., Thomson, S., Marsh, M., Kay, J., Weiss, R. A. & Moore, J. P. (1991) *AIDS Res. Hum. Retroviruses* **7,** 3–15.
17. Gupta, G. & Meyers, G. (1990) *Computer Analysis of HIV Epitope Sequences 1-99-105* (Pasteur Vaccins, Paris).
18. Veronese, F. D. M., Jr., M. S. R., Gupta, G., Robert-Guroff, M., Boyer-Thompson, C., Gallo, R. C. & Lusso, P. (1993) *J. Biol. Chem.* **268,** 25894–25901.
19. Gupta, G., Anantharamaiah, G. M., Scott, D. R., Eldridge, J. H. & Myers, G. (1993) *J. Biomol. Struct. Dyn.* **11,** 345–366.
20. Gupta, G. & Myers, G. (1994) in *Peptides: Design, Synthesis, and Biological Activity*, eds. Basava, C. & Anantharamaiah, G. M. (Birkhauser, Boston), pp. 259–277.
21. Rini, J. M., Stanfield, R. L., Stura, E. A., Salinas, P. A., Profy, A. T. & Wilson, I. A. (1993) *Proc. Natl. Acad. Sci. USA* **90,** 6325–6329.
22. Ghiara, J. B., Stura, E. A., Stanfield, R. L., Profy, A. T. & Wilson, I. A. (1994) *Science* **264,** 82–85.
23. Gendler, S., Taylor-Papadimitriou, J., Duhlig, T., Rothbard, J. & Burchell, J. A. (1988) *J. Biol. Chem.* **263,** 12820–12823.
24. Jerome, K. R., Barnd, D. L., Bendt, K. M., Boyer, C. M., Taylor-Papadimitriou, J., McKenzie, I. F. C., Bast, R. C., Jr., & Finn, O. J. (1991) *Cancer Res.* **51,** 2908–2916.
25. Fontenot, J. D., Tjandra, N., Bu, D., Ho, C., Montelaro, R. C. & Finn, O. J. (1993) *Cancer Res.* **53,** 5386–5394.
26. Fontenot, J. D., Finn, O. J., Dales, N., Andrews, P. C. & Montelaro, R. C. (1993) *Pept. Res.* **6,** 330–336.
27. Pau, C. P., Lee-Thomas, S., Auwanit, W., George, J. R., Ou, C. Y., Parekh, B. S., Granade, T. C., Holloman, D. L., Phillips, S., Schochetman, G., Young, N. L., Takebe, Y., Gayle, H. D. & Weniger, B. G. (1993) *AIDS* **7,** 337–340.
28. Bax, A. & Davis, D. G. (1985) *J. Magn. Reson.* **63,** 207–213.
29. Jeener, J., Meier, B. H., Bachman, P. & Ernst, R. R. (1979) *J. Chem. Phys.* **71,** 4546–4553.
30. Nemethy, G., Pottle, M. S. & Scheraga, H. A. (1983) *J. Phys. Chem.* **87,** 1883–1887.
31. Kirkpatrick, S., Jr., Gelatt, C. D., Jr., & Vecchi, M. P. (1983) *Science* **220,** 671–680.
32. Taylor-Papadimitriou, J. (1991) *Int. J. Cancer* **49,** 1–5.
33. Devine, P. L. & McKenzie, I. F. C. (1992) *BioEssays* **14,** 619–625.
34. Rose, D. R., Gierasch, L. M. & Smith, J. A. (1985) *Adv. Protein Chem.* **37,** 1–109.
35. Lorimer, R. D., Moody, M. A., Haynes, B. F. & Spicer, L. D. (1994) *Biochemistry* **33,** 2055–2062.
36. Gupta, G., Sarma, M. H. & Sarma, R. H. (1988) *Biochemistry* **27,** 3423–3431.
37. D'Souza, M. P., Durda, P., Hanson, C. V. & Milman, G. (1991) *AIDS* **5,** 1061–1070.
38. Catasti, P., Fontenot, J. D., Bradbury, E. M. & Gupta, G. (1995) *J. Biol. Chem.*, in press.